

Quantifying and Predicting the Tensile Properties of Silicone Reinforced with *Moringa oleifera* Bark Fibers

Mohd Nor Azmi Ab Patar,^a Nur Aini Sabrin Manssor,^b Mohd Rashdan Isa,^c Nur Auni Izzati Jusoh,^a Mohd Juzaila Abd Latif,^d Praveena N. Sivasankaran,^e and Jamaluddin Mahmud^{a,*}

To obtain a better understanding of using *Moringa oleifera* bark (MOB) as a reinforcement in a silicone matrix, this study aimed to define the mechanical properties of this new material under uniaxial tension. Composite samples of 0 wt%, 4 wt%, 8 wt%, 12 wt%, and 16 wt% MOB powder were produced. The tensile properties were quantified mathematically using the neo-Hookean hyperelastic model. The collected data were employed to establish multiple inputs of an artificial neural network (ANN) to predict its material constant *via* MATLAB. The result showed that the material constant for the 16 wt% fiber content sample was 63.9% higher than pure silicone. This was supported by the tensile modulus testing, which indicated that the modulus increased as the fiber content increased. However, the elongation ratio (λ) of the MOB-silicone biocomposite decreased slightly compared to the pure silicone. Lastly, the prediction of the material constant using an ANN recorded a 2.03% percentage error, which showed that it was comparable to the mathematical modelling. Therefore, the inclusion of MOB fibers into silicone produced a stiffer material and gradually improved the composite. Furthermore, the network that had multiple inputs (weighting, load, and elongation) was more reliable to produce precise predictions.

DOI: 10.15376/biores.19.2.3461-3474

Keywords: *Moringa oleifera*; Silicone biocomposite; Tensile properties; Artificial neural network; Neo-Hookean hyperelastic model

Contact information: a: School of Mechanical Engineering, College of Engineering, Universiti Teknologi MARA, 40450, Selangor, Malaysia; b: College of Engineering, Universiti Teknologi MARA Johor Branch, Pasir Gudang Campus, 81750 Masai, Johor, Malaysia; c: Department of Mechanical Engineering, College of Engineering, Universiti Tenaga Nasional, 43000 Kajang, Selangor, Malaysia; d: Fakulti Teknologi dan Kejuruteraan Mekanikal, Universiti Teknikal Malaysia Melaka, 76100 Durian Tunggal, Melaka, Malaysia; e: GV Medhini Consultancy & Resources Sdn Bhd, Periwinkle, 42500 Bandar Rimbayu, Selangor, Malaysia; * Corresponding author: jm@uitm.edu.my

INTRODUCTION

The unique properties of composite materials facilitate their use in modern structures. Composite materials are comprised of two or more constituent materials to form a single useful body (Rajak *et al.* 2019). Biocomposite materials are made from the combination of a matrix (resin) with natural fibers. This combination of a matrix and the reinforcement of biomaterial can create a new material that meets the requirements of industrial applications in the aerospace, automotive, construction, sports, and biomedical, fields, among others (Bharath and Basavarajappa 2016; Keya *et al.* 2019).

As technology improves, the materials of composites also need to evolve. Hence, many researchers have successfully produced composite materials using natural fibers with comparable properties to synthetic fibers. For example, Chandramohan and Bharanichandar (2014) produced a roof frame for a car from a natural fiber composite. The component possessed lightweight and heat resistance properties, and it was seen as a suitable replacement for synthetic fibers, such as phenolic resin fiber.

Many types of natural fibers have been the subject of previous research. Natural fibers can be identified in several groups such as from animal (silk, wool, and hair), vegetable (leaf, seed, wood, baste, hemp, and jute), and mineral (asbestos) (Bharath and Basavarajappa 2016; Keya *et al.* 2019). The use of natural fibers in industrial applications is common due to their lightweight properties, low cost, and abundance (Bharath and Basavarajappa 2016). Natural fibers are alternative resources to synthetic fibers, such as glass and carbon fibers, which are generally non-renewable, non-biodegradable, and expensive (Rajak *et al.* 2019). In addition, the production of materials such as coal and aramid can be hazardous to human health and the environment (Muneer 2015). Therefore, the use of natural fibers in composites is preferable because they are safer and environmentally friendly compared to conventional reinforcement materials.

Moringa oleifera bark (MOB) is a natural fiber from the vegetable group. The MO plant is also known as the “tree of life” or the “miracle tree.” The natives of India called the MO plant “*Shajna*,” which is due to the fact that the plant has an abundance of nutrients in its leaves, pods, and seeds that are medically valuable (Taher *et al.* 2017). The MO plant is recognized as a valuable source of special medicines for various diseases. *Moringa oleifera* has drought-tolerant properties that allow it to grow in places like Ethiopia, the Pacific Islands, Florida, Sudan, the Caribbean, the Philippines, South Africa, Asia, and Latin America (Daba 2016). The height range of the tree is from 5 m to 12 m and its fruits (pods) are approximately 50 cm long (Taher *et al.* 2017). In fact, the leaves of MO have a wide range of uses, such as food for human consumption, medicine, dye, soil and water conservation, livestock forage, and green manure (Daba 2016).

According to previous studies, the high alkaloid content in MOB can eventually remove acidity in stomach ulcers and treat ulceration. The bark itself can also be used as a cardiac stimulant, and an anti-ulcer and anti-inflammatory agent due to an abundance of alkaloids (morphine and moriginine) and minerals (calcium, magnesium, and sodium) (Choudhary *et al.* 2013; Gopalakrishnan *et al.* 2016; Taher *et al.* 2017; Liu *et al.* 2018). Furthermore, according to a study by George *et al.* (2016), MOB can remove metal ions from contaminated water and can eventually be used as an alternative sorbent agent. *Moringa oleifera* bark has good metal absorption capacity by weakening the heavy metal biomass linkage.

Although there has been extensive research on the leaves and seeds of MO, there is little data on the tensile behavior of MOB. Therefore, this research was carried out to fabricate a new silicone biocomposite material that can reinforce the MOB powder into silicone rubber. The goal of this work was to explain and analyze the tensile behavior of MOB-silicone biocomposites under uniaxial tensile load, where it was quantified using hyperelastic constitutive models (neo-Hookean).

Specimen Setup

The MO stem was obtained from local people in Kota Kemuning, Selangor, Malaysia. The stem of the MO tree was cut approximately 10 cm long, and the barks were

peeled off from the stem. The barks were washed and rinsed with water to remove the dirt or any contaminant particles. The MOB was dried on a tray in an oven at 100 °C for 24 h. The dried bark was cooled at room temperature before it was crushed into small chips using a crusher machine (SCP, Shah Alam, Malaysia).

The crushed barks were milled using a planetary mono mill machine (Pulverisette 6 classic line; Fritsch, Idar-Oberstein, Germany) at 270 revolutions per min for 30 min four times. The weight of the milling ball was decided based on a 1:2 ratio with 1 (MOB): 2 (milling ball). Then, the MOB was sieved at 150 μm using a vibratory sieve shaker (Fritsch, Idar-Oberstein, Germany) to get the fine powdered MOB. Once the fiber was sieved into fine powder, the density of the fiber was measured using a Micromeritics pycnometer (AccuPyc II 1340; Norcross, GA, USA) at a pressure of 20 psi. The MOB powder had a density of 1.562 g/cm^3 .

The platinum cure silicone rubber compound was obtained from Castmech Technologies (Silicone EcoFlex 00-30, Ipoh, Malaysia). The product is in liquid form and consists of Part A and Part B to be mixed accordingly following instructions provided by the manufacturer to produce silicone rubber solution. The specimens were prepared at MOB fiber content levels of 0 wt%, 4 wt%, 8 wt%, 12 wt%, and 16 wt%. Five samples were produced for each content level to produce 25 samples in total. The measured weight of MOB powder was mixed with the silicone rubber solution, and the mixture was stirred constantly using a wooden stick. It is vital to ensure homogeneity by stirring the mixture consistently to avoid accumulated fibers in the mixture. Lastly, the mixture was poured into pre-made dumbbell-shaped mould made of aluminium plate and cured at room temperature for approximately 4 h. The procedure was conducted following precisely, as in the previous work by Bahrain and Mahmud (2019), which reported good dispersion of fibers without traces of agglomeration (Bahrain and Mahmud 2019; Bahrain *et al.* 2022).

Mechanical Testing

The samples were fabricated into a dumbbell shape (Fig. 1) with a thickness of 3 mm, in accordance with the ASTM D412 (2016) standard. The tensile strength was measured with an Instron universal testing machine (3382 Universal Testing Machine 100 kN; Norwood, MA, USA). The uniaxial load testing was done using a load cell of 100 kN at a speed of 500 mm/min.

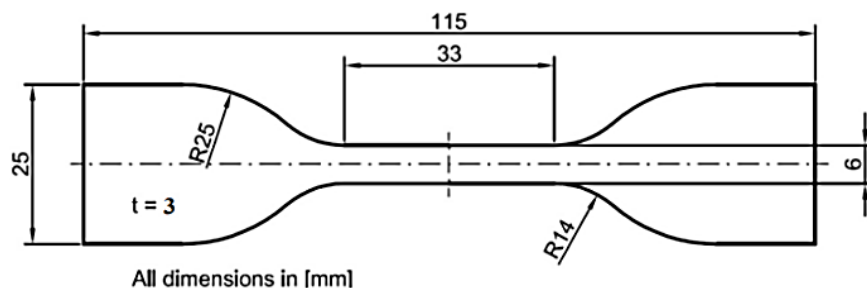


Fig. 1. A diagram of the specimen dimensions

Quantifying Tensile Properties

Silicone material exhibits a nonlinear stress-strain curve. Therefore, the data gained from the tensile test was quantified to observe the tensile behavior of the specimen. The specimen was quantified using the neo-Hookean model, where it was solved by a

mathematical equation to determine the material constants of the silicone biocomposite sample. The quantification of the sample was done according to Eq. 1,

$$\sigma_E = (2 C_1) \left(\lambda - \frac{1}{\lambda^2} \right) \quad (1)$$

where σ_E is the engineering stress (kPa), C_1 is the material constant (kPa), and λ is the extension ratio (stretch ratio). The experimental material constant, C_1 , was obtained by solving Eq. 1 using the “solver tool” in Microsoft Excel (version 2019, Redmond, WA, USA).

The extension ratio is defined as the ratio of stretched length to unstretched length. The extension ratio was determined by Eq. 2,

$$\lambda = \varepsilon + 1 \quad (2)$$

where ε is the strain, which was obtained from the interpolation of the tensile data.

RESULTS AND DISCUSSION

Tensile Properties

Based on the plotted graph in Fig. 2, the pure silicone (0 wt%) exhibited a slightly nonlinear elastic behavior with concave upward pattern in comparison to the other four specimens. The addition of the MOB fibers has affected the curve trends, which caused them to behave more linearly as the fiber content increased (up to the breaking point).

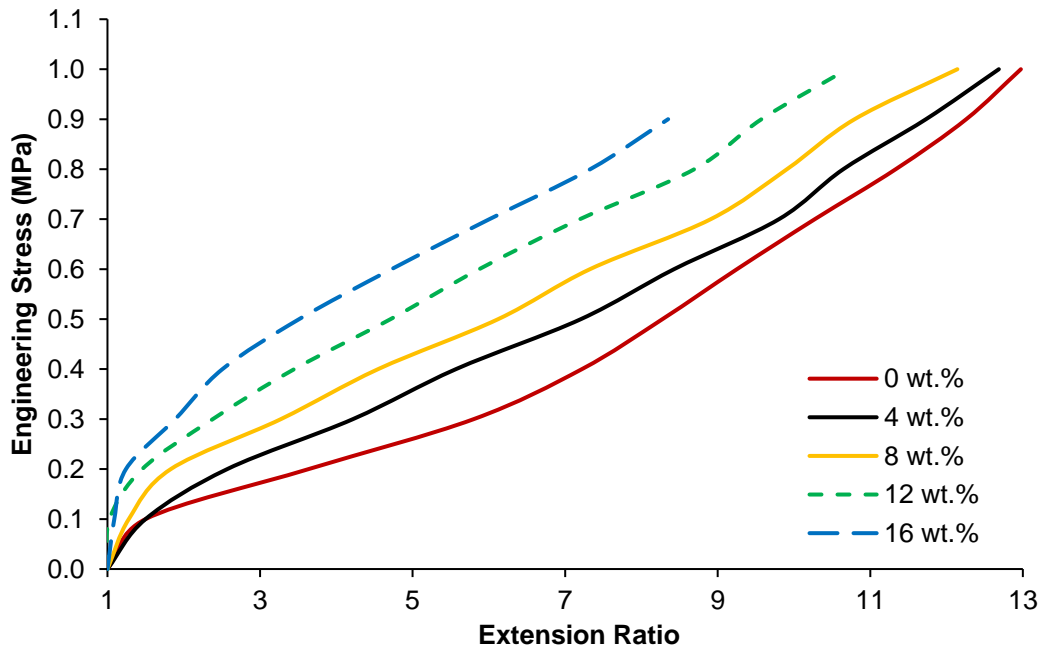


Fig. 2. The engineering stress-extension ratio for the average values of the MOB-silicone biocomposites compared to the pure silicone

Furthermore, the pure silicone also recorded the highest stretch, as it elongated the most to reach the breaking point. The material constant value in Table 1 shows the average tensile properties for the MOB-silicone biocomposites and the pure silicone.

Table 1. The Average Tensile Properties of the MOB-silicone Biocomposites

MOB Addition (wt%)	Material Constant, C_1 (kPa)	Maximum Elongation Ratio
0	36	11.07 ± 1.08
4	37	11.99 ± 0.83
8	41	10.93 ± 0.84
12	48	10.14 ± 0.75
16	59	8.01 ± 0.62

As shown in Table 1, the 16 wt% sample possessed the highest material constant and the lowest elongation point, at 59 kPa and 8.01, respectively. The specimens became more rigid as the fiber content increased. This may be attributed to the fibers strengthening the structure as they filled the gap in the matrix chains in the composite. Similar findings have been reported by Jusoh *et al.* (2023), Noor Haris *et al.* (2022), and Bahrain *et al.* (2022) based on their morphological analysis. In particular, Bahrain *et al.* (2022) highlighted that pure silicon rubber had a smooth and flat surface, which explained its low resistance to deformation, while the addition of fibers revealed a rough surface as the fracture is forced to propagate in between the fibers, thus resist the breaking during tensile loading. A higher material constant value was correlated with stiffer material behavior under tensile load, as the samples exhibited lower elongation at break values.

In previous research on hyperelastic behavior, the kenaf-silicone composite (Azmi *et al.* 2017) and *Arenga pinnata*-silicone biocomposite (Bahrain and Mahmud 2019) were discovered to have similar behaviors. As the percentage of reinforced fiber in the composites increased, the value of the material constant increased. The material constant of the MOB-silicone composite was greater than that of these two materials and values were comparable with *Hevea brasiliensis* silicone biocomposites, as summarized in Table 2. This indicated that the MOB-silicone composite had better tensile properties than other biocomposites.

Table 2. Comparison of Material Constant Value of Current Study with Previous Research

Material constant (C_1)	Material Type	Reference
45 to 78 kPa	<i>Hevea brasiliensis</i> silicone biocomposite	Noor Haris <i>et al.</i> (2022)
41.7 kPa	Silicone EcoFlex 00-30	Current study
37.4 to 58.8 kPa	<i>Moringa oleifera</i> bark – silicone biocomposite	Current study
32 to 53 kPa	Kenaf silicone biocomposite	Noor <i>et al.</i> (2015)
31.7 to 47 kPa	<i>Curcuma longa</i> silicone biocomposite	Zainal Abidin <i>et al.</i> (2022)
22 kPa to 74 kPa	<i>Arenga pinata</i> silicone biocomposite	Bahrain <i>et al.</i> (2018)

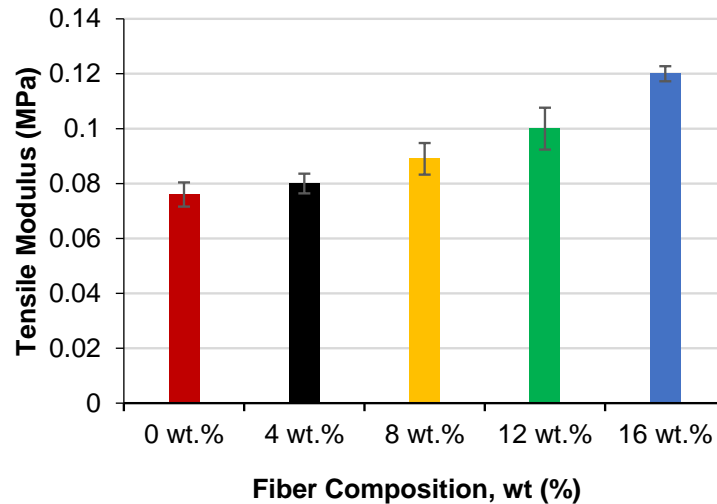


Fig. 3. The average tensile modulus values of the MOB-silicone biocomposites

As can be seen in Fig. 3, the inclusion of the MOB fiber in the silicone rubber increased the tensile modulus values of the biocomposites. A stiff material has a high modulus of elasticity and will only experience slight changes to its shape under elastic loads. Therefore, increasing the MOB content in the silicone rubber will increase the stiffness of the material.

These findings are in agreement with a study by Koushki *et al.* (2020), where the addition of hemp fiber increased the stiffness of the silicone composites. Similarly, the composite stiffness in this study increased as the fiber addition rate increased. In the study by Koushki *et al.* (2020), the modulus of elasticity of the silicone composite increased from 2 to 7.5 MPa as the hemp fiber addition level was increased from 0% and 20%, respectively. In addition, the incorporation of fiber can also affect the elongation at break properties of the composite. Koushki *et al.* (2020) found that a higher fiber concentration will restrict the molecular motion of the composite, thereby reducing the ductility.

Sarath *et al.* (2020) found a similar pattern regarding the modulus of elasticity on exfoliated graphite (EG)-silicone rubber. The modulus of elasticity of the EG-silicone composite increased as the EG content was increased. The sample with the lowest EG content in the silicone composite exhibited the highest elongation before breakage. The 0 parts per hundred parts of rubber (phr) EG sample had an elongation of 198%. Meanwhile, the 15 phr EG sample had an elongation of 143%. Therefore, a higher fiber content in the matrix will produce a stiffer material.

The tensile modulus defines the resistance of the material towards elastic deformation under tensile load. In other words, a material that has a high tensile modulus value indicates that it is a stiffer material. As shown in Table 1, the 16 wt.% MOB-silicone biocomposite sample had the highest C_1 value, at 59 kPa. This indicated that the increased tensile modulus was due to the high fiber content in the silicone rubber matrix, which produced a stiffer composite.

Predicted Tensile Properties

The networks were trained using 15 data tests, while another 10 data tests were used to validate the network. Figure 4 shows the view of the neural predicting, which consisted of two inputs and one output. The inputs used in this network were weighting

and load, while the output was the predicted C_1 value. The predicted values were then compared with the target values, as shown in Table 3, which were recorded from the solver tool. Figure 4 shows the schematic diagram of Network 1.

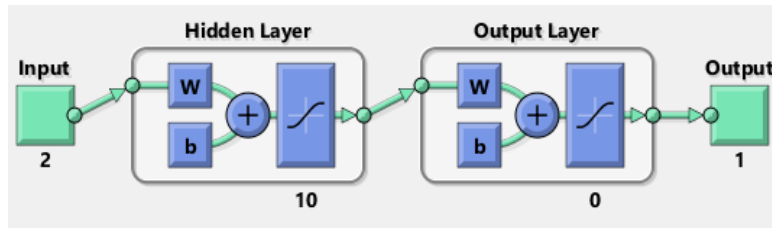


Fig. 4. The schematic diagram of Network 1 with two inputs (weightage and load) and one output (material constant, C_1 value)

This neural net was named Network 1. The error values in Table 3 were calculated based on the target and output values for each sample. For the 0 wt% composite, the error percentage for sample 1 had a higher value compared to sample 5, at 1.69% and 0.77%, respectively. This was due to the difference in the material constant and maximum load values, which contributed to the increment of error. In terms of strain, sample 1 initially stretched more as the load increased before breaking. This also occurred in the 4 wt% and 16 wt% MOB-silicone biocomposites.

As shown in Table 3, the artificial neural network (ANN) prediction deposition rate was close to the range of experimental value, with a maximum error range of $\pm 3\%$. The training data for the 12 wt% had a high difference value between the targeted and output values. The targeted values for sample 1 and sample 5 were 51 and 47 kPa, respectively. The output values for sample 1 and sample 5 were 44 and 53 kPa, respectively. This caused the error rate to increase 13.47% and 12.16% for sample 1 and sample 5, respectively.

Table 3. The Error Percentage Error (%) and Material Constant (MPa) Output of the Neural Network (Network 1) MOB-Silicone Biocomposites

INPUT		TARGET	OUTPUT	ERROR (%)
MOB Addition (wt%)	Max Load (N)	Material Constant, C_1 (kPa)		
0	19.628	34.482	33.9	1.69
0	15.098	33.244	33.5	0.77
4	18.381	37.043	36.7	0.93
4	16.347	36.682	35.5	3.22
8	17.873	44.825	40.3	10.09
8	17.266	38.221	39.4	3.08
12	17.220	50.619	43.8	13.47
12	19.219	47.344	53.1	12.16
16	15.050	57.140	54.5	4.62
16	17.828	62.605	59.8	4.48

Figure 5 shows the regression plot gained from Network 1, which represented training, validation, testing, and overall data. The x-axis refers to the C_1 value and the y-axis represents the value of the predicted C_1 value by the trained network. The dotted line represents the best correlation between the target and the output, while the colored lines represent the actual correlation of the network.

The correlation coefficient (R) for the training was 0.99854 and the overall R value was 0.99203. Meanwhile, the R value for the validation and test set was equal to one. If R is equal to one, the slope has a perfect fit (output is exactly equal to the target), only if y intercepts at 0. However, the y-intercept for both slope in validation and test was not equal to zero, as illustrated in Fig. 5.

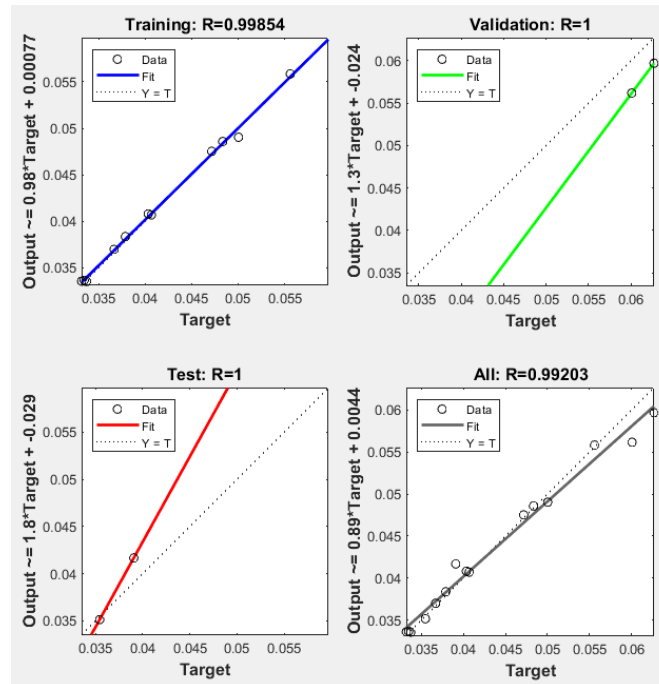


Fig. 5. The regression plot of the ANN for Network 1

Vineela *et al.* (2018) reported a similar regression plot pattern in predicting the tensile strength of hybrid composites. It was determined that the phenomena occurred because of insufficient data points during the training network. Therefore, the authors created a new network by inserting more data points in the training process to obtain better correlation coefficient values. The correlation coefficient values for the train, test, and validation data sets should be similar. If these correlation coefficient values have small differences, it indicates high accuracy to the network, as observed in the prediction results from previous studies (Ghritlahre and Prasad 2017; Vineela *et al.* 2018; Mohammadi *et al.* 2020).

As shown in Fig. 6, the results from this study had a high percentage of error, in which the best validation performance value of the mean squared error (MSE) was $1.214e^{-5}$ at epoch 5. Therefore, the network needs to be trained with more data to develop a concrete network that can precisely predict C_1 .

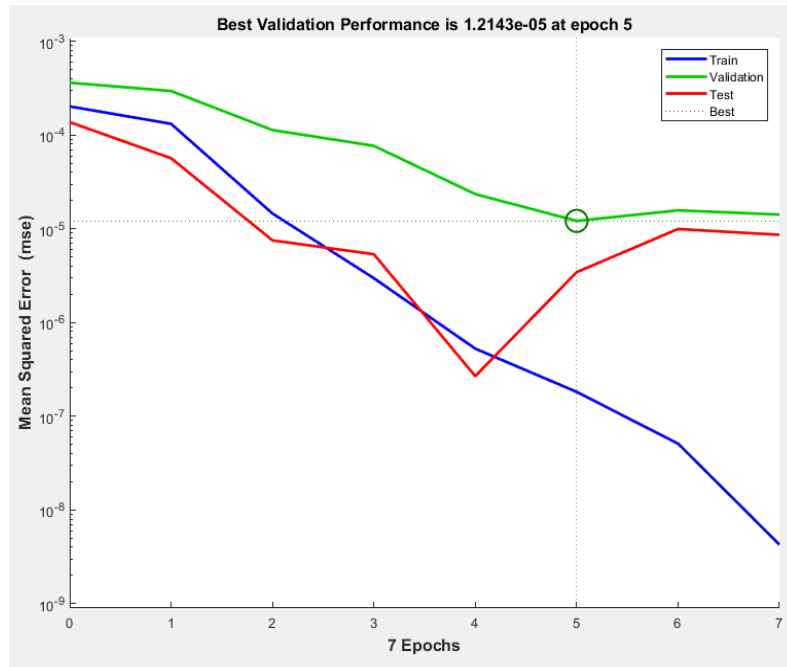


Fig. 6. The performance plot of the ANN for Network1

Improved Network

Generally, the Network 1 was considered to have a large percentage error range because it only had two data group inputs. Therefore, the network was improvised by adding more data into the input group where it consisted of three data groups which were weighting, load, and elongation. This improvised network was named Network 2, while the previous network was named Network 1.

The input was then solved by a computational system to predict one output, the C_1 value of the silicone biocomposite. Figure 7 shows the schematic diagram of the neural network for Network 2. In this network, 20 data tests were used to train the network and five data tests were used to validate the network. This was done to increase the variation of the set of data tested. This also increased the accuracy of the predicted C_1 on the network.

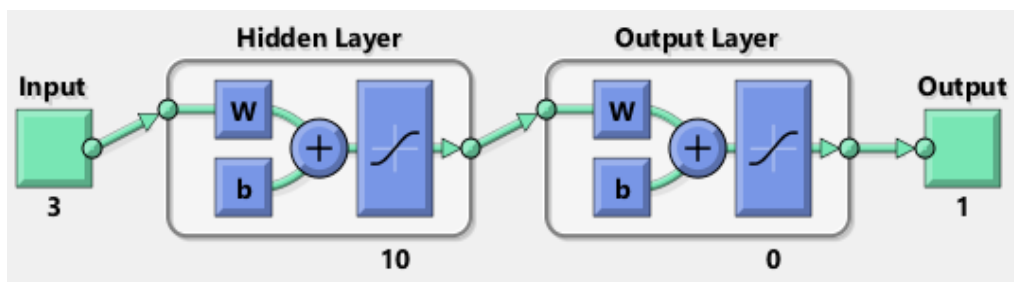


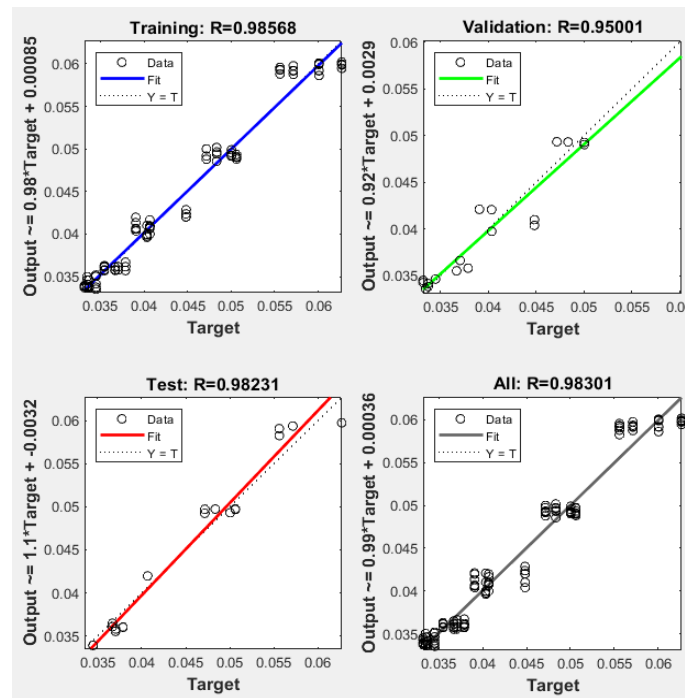
Fig. 7. The schematic diagram of Network 2 with three inputs (weighting, load, and elongation) and one output (material constant, C_1 value)

Table 4. Comparison of the Percentage Error Between Network 1 and Network 2 for the MOB-silicone Biocomposites

INPUT			TARGET	OUTPUT	ERROR (%)	
MOB Addition (wt%)	Load (N)	Elongation (mm)	Material Constant, C_1 (kPa)		Network 1	Network 2
0	15.09846	300.83	33.2444	33.8	1.69	1.67
4	16.34666	334.17	36.6819	36.7	3.22	0.049
8	17.26647	363.33	38.2214	39.3	3.08	2.822
12	19.21898	342.50	47.3436	46.2	12.16	2.416
16	17.82843	250.83	62.6047	60.6	4.48	3.202
MAPE					4.926	2.032

As shown in Table 4, the percentage error of the MOB-silicone biocomposite in Network 2 revealed a reduction in all the weighting samples. The 12 wt% specimen showed a reduction in the error, from 12.16% to 2.416%. In terms of performance, the mean absolute percentage error (MAPE) was calculated for both networks to differentiate the effectiveness between Network 1 and Network 2. If the value of the MAPE is high, the network is considered unable to precisely predict the C_1 . As seen in Table 4, Network 2 had a small MAPE value (2.032%) compared to Network 1 (4.926%). This means that Network 1 provides low accuracy in the prediction of the C_1 values.

Figure 8 represents the regression plot for training, validation, testing, and overall data for Network 2. Each slope in training, validation, testing, and overall data were seen to have interception on y-axis as it revealed that the network had undergone a good training process. The R values for training, validation, testing, and overall data were recorded at 0.98568, 0.95001, 0.98231, and 0.98301, respectively.

**Fig. 8.** Regression plots of ANN for Network2

The validation performance of Network 2 (Fig. 9) displayed a good curve compared to Network 1 (Fig. 6). As seen in Fig. 9, the line curve of Network 2 was uniform, which indicated that the training had no major problems. The line curve for Network 1 in Fig. 6 was quite far from the dotted line. This shows that Network 1 did not accurately predict the output, which produced a high MAPE value in the predicting process.

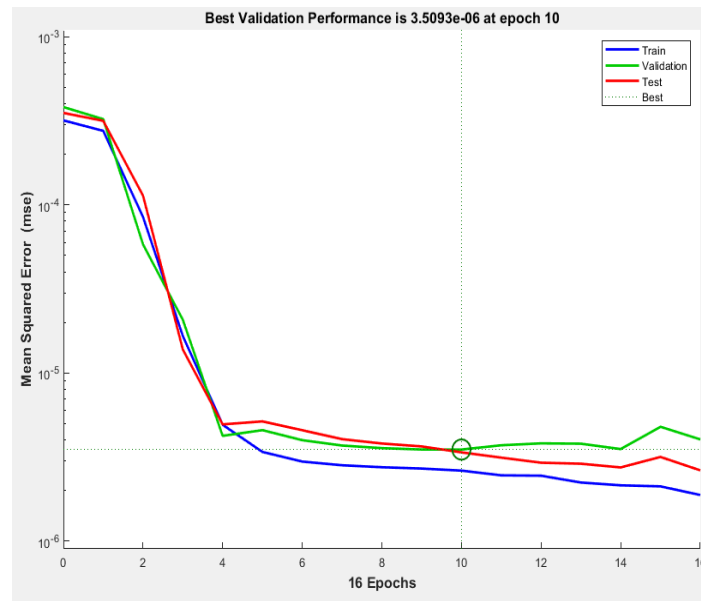


Fig. 9. The performance plot of the ANN for Network 2

Supeni *et al.* (2014) reported that the validation performance in their study was improved when they added more data in the training network process. The network was constructed to predict the performance of a smart wind turbine blade. The network improved as it showed a small MSE value in the validation performance graph after training the network. It was found that when the value of the MSE was near zero, the network was a well-trained model. From Figs. 6 and 9, the MSE value gained from Network 1 was $1.214e^{-5}$ at epoch 5, while Network 2 was $3.509e^{-6}$ at epoch 10. Network 2 has the nearest value to zero, which means Network 2 was closer to a perfect prediction model than Network 1.

In a study by Ghritlahre and Prasad (2017), networks to predict the thermal performance of a bed solar air heater were constructed. Several networks were created using different training functions with the same data to make a comparison of the performance between each training function. Comparisons were made based on the gained values such as the root mean square error (RMSE), MSE, and coefficient of determination (R^2). The training function with the lowest MSE value was selected as the best function. The study also stated that the R values for training, validation, testing, and overall data had similar values which were 0.99985, 0.99991, 0.99958, and 0.9998, respectively.

Therefore, this study showed that Network 2 was a more accurate network than Network 1. Using multiple inputs in the training phase produced better ANN prediction, which was in agreement with a previous study (Jami *et al.* 2012). The additional data in the training process has improved the network to do recognition pattern in predicting the tensile values based on experimental data.

CONCLUSIONS

1. This study demonstrated the tensile properties of a potential new type of biocomposite materials by reinforcing silicone rubber with the bark of *Moringa oleifera* (MO). The experimental data variation was adequate for all the samples.
2. The *Moringa oleifera* bark (MOB) influenced the tensile properties and the material constant C_1 of the silicon rubber. As the MOB addition rate increased, the tensile modulus and C_1 increased through the reinforcement of fiber.
3. The MOB-silicone biocomposite was successfully evaluated using the neo-Hookean model and the artificial neural net (ANN) model. It was shown that the material constant in both models were comparable with a low error percentage. As more training data was utilized, the network was more accurately able to predict the material constant.
4. Future research on the density and moisture absorption behavior of MOB-silicone biocomposites is required to have a better understanding of their potential and practical applications.

ACKNOWLEDGMENTS

This work was supported by Universiti Teknologi MARA (Skim Geran Insentif Penyelidikan, Grant no. 600-RMC/GIP 5/3 (101/2023)).

REFERENCES CITED

- ASTM D412 (2016). "Standard test methods for vulcanized rubber and thermoplastic elastomers—Tension," ASTM International, West Conshohocken, PA.
- Azmi, N. N., Hussain, A. K., and Mahmud, J. (2017). "Kenaf silicone biocomposites: Synthesis and its hyperelastic behaviour," *Materials Science Forum* 900, 12-16. DOI: 10.4028/www.scientific.net/MSF.900.12
- Bahrain, S. H. K., and Mahmud, J. (2019). "Swelling behaviour and morphological analysis of *Arenga pinnata*–silicone biocomposite," *Materials Letters* 242, 32-34. DOI: 10.1016/j.matlet.2019.01.100
- Bahrain, S. H. K., Mahmud, J., and Ismail, M.H. (2018). "*Arenga pinnata*–Silicone biocomposite properties via experimental and numerical analysis," *Materials Science (Medziagotyra)* 24(3), 277-282. DOI: 10.5755/j01.ms.24.3.18296
- Bahrain, S. H. K., Masdek, N. R. N., Mahmud, J., Mohammed, M. N., Sapuan, S. M., Ilyas, R. A., Mohamed, A., Shamseldin, M. A., Abdelrahman, A., and Asyraf, M. R. M. (2022). "Morphological, physical, and mechanical properties of sugar-palm (*Arenga pinnata* (Wurmb) Merr.)-reinforced silicone rubber biocomposites," *Materials* 15(12). DOI: 10.3390/ma15124062
- Bharath, K. N., and Basavarajappa, S. (2016). "Applications of biocomposite materials based on natural fibers from renewable resources: A review," *Science and Engineering of Composite Materials* 23(2), 123-133. DOI: 10.1515/secm-2014-0088

- Chandramohan, D., and Bharanichandar, J. (2014). "Natural fiber reinforced polymer composites for automobile accessories," *American Journal of Environmental Science* 9(6), 494-504. DOI: 10.3844/ajessp.2013.494.504
- Choudhary, M. K., Bodakhe, S. H., and Gupta, S. K. (2013). "Assessment of the antiulcer potential of *Moringa oleifera* root-bark extract in rats," *Journal of Acupuncture and Meridian Studies* 6(4), 214-220. DOI: 10.1016/j.jams.2013.07.003
- Daba, M. (2016). "Miracle tree: A review on multi-purposes of *Moringa oleifera* and its implication for climate change mitigation," *Journal of Earth Science & Climatic Change* 7(8), article 366. DOI: 10.4172/2157-7617.1000366
- George, K. S., Revathi, K. B., Deepa, N., Sheregar, C. P., Ashwini, T. S., and Das, S. (2016). "A study on the potential of moringa leaf and bark extract in bioremediation of heavy metals from water collected from various lakes in Bangalore," *Procedia Environmental Sciences* 35, 869-880. DOI: 10.1016/j.proenv.2016.07.104
- Ghritlahre, H. K., and Prasad, R. K. (2017). "Prediction of thermal performance of unidirectional flow porous bed solar air heater with optimal training function using artificial neural network," *Energy Procedia* 109, 369-376. DOI: 10.1016/j.egypro.2017.03.033
- Gopalakrishnan, L., Doriya, K., and Kumar, D. S. (2016). "*Moringa oleifera*: A review on nutritive importance and its medicinal application," *Food Science and Human Wellness* 5(2), 49-56. DOI: 10.1016/j.fshw.2016.04.001
- Jami, M. S., Husain, I. A. F., Kabashi, N. A., and Abdullah, N. (2012). "Multiple inputs artificial neural network model for the prediction of wastewater treatment plant performance," *Australian Journal of Basic and Applied Sciences* 6(1), 62-69. DOI: 10.2316/P.2011.736-050
- Jusoh, N. A. I., Manssor, N. A. S., Rajendra, P. N., and Mahmud, J. (2023). "The effect of reinforcing moringa oleifera bark fibre on the tensile and deformation behaviour of epoxy and silicone rubber composites," *Pertanika Journal of Science and Technology* 31(4), 1895-1910. DOI: 10.47836/pjst.31.4.17
- Keya, K. N., Kona, N. A., Koly, F. A., Maraz, K. M., Islam, N., and Khan, R. A. (2019). "Natural fiber reinforced polymer composites: History, types, advantages, and applications," *Materials Engineering Research* 1(2), 69-87. DOI: 10.25082/mer.2019.02.006
- Koushki, P., Kwok, T.-H., Hof, L., and Wuthrich, R. (2020). "Reinforcing silicone with hemp fiber for additive manufacturing," *Composites Science and Technology* 194, article 108139. DOI: 10.1016/j.compscitech.2020.108139
- Liu, Y., Wang, X.-y., Wei, X.-m., Gao, Z.-t., and Han, J.-p. (2018). "Values, properties and utility of different parts of *Moringa oleifera*: An overview," *Chinese Herbal Medicines* 10(4), 371-378. DOI: 10.1016/j.chmed.2018.09.002
- Mohammadi, F., Bina, B., Karimi, H., Rahimi, S., and Yavari, Z. (2020). "Modeling and sensitivity analysis of the alkylphenols removal via moving bed biofilm reactor using artificial neural networks: Comparison of Levenberg Marquardt and particle swarm optimization training algorithms," *Biochemical Engineering Journal* 161, article 107685. DOI: 10.1016/j.bej.2020.107685
- Muneer, F. (2015). "Biocomposites from natural polymers and fibers," *Introductory Paper at the Faculty of Landscape Architecture, Horticulture and Crop Production Science* 3, 4-30.

- Noor Haris, N. F., Yahaya, M. A., and Mahmud, J. (2022). "Tensile properties of silicone biocomposite reinforced with waste material (*Hevea brasiliensis* sawdust): Experimental and numerical approach," *BioResources* 17(3), 4623-4637. DOI: 10.15376/biores.17.3.4623-4637
- Noor, S. N. A. M., Khairuddin, M. A. F., and Mahmud, J. (2015). "Biocomposite silicone: Synthesis, mechanical testing and analysis," *New Developments in Mechanics and Mechanical Engineering* 1(1), 113-117.
- Rajak, D. K., Pagar, D. D., Kumar, R., and Pruncu, C. I. (2019). "Recent progress of reinforcement materials: A comprehensive overview of composite materials," *Journal of Materials Research and Technology* 8(6), 6354-6374. DOI: 10.1016/j.jmrt.2019.09.068
- Sarath, P. S., Samson, S. V., Reghunath, R., Pandey, M. K., Haponiuk, J. T., Thomas, S., and George, S. C. (2020). "Fabrication of exfoliated graphite reinforced silicone rubber composites - Mechanical, tribological and dielectric properties," *Polymer Testing* 89, article 106601. DOI: 10.1016/j.polymertesting.2020.106601
- Supeni, E. E., Epaarachchi, J. A., Islam, M. M., and Lau, K. T. (2014). "Development of artificial neural network model in predicting performance of the smart wind turbine blade," *Journal of Mechanical Engineering and Sciences* 6, 734-745. DOI: 10.15282/jmes.6.2014.1.0071
- Taher, M. A. Nyeem, M. A. B., Ahammed, M., Hossain, M., and Islam, M. N. (2017). "*Moringa oleifera* (Shajna): The wonderful indigenous medicinal plant," *Asian Journal of Medical and Biological Research* 3(1), 20-30. DOI: 10.3329/ajmbr.v3i1.32032
- Vineela, M. G., Dave, A., and Chaganti, P. K. (2018). "Artificial neural network based prediction of tensile strength of hybrid composites," *Materials Today: Proceedings* 5(9), 19908-19915. DOI: 10.1016/j.matpr.2018.06.356
- Zainal Abidin, N. A., Mahmud, J., Manssor, N. A. S., and Che Abd Rahim, N. N. (2022). "Physical and mechanical properties of bamboo-silicone biocomposites (BaSiCs)," *BioResources* 17(3), 4432-4443. DOI: 10.15376/biores.17.3.4432-4443

Article submitted: April 21, 2022; Peer review completed: July 17, 2022; Revised version received: March 30, 2024; Published: April 17, 2024.

DOI: 10.15376/biores.19.2.3461-3474